Natural Hazards (2022) 114:127–156
https://doi.org/10.1007/s11069-022-05383-y

ORIGINAL PAPER

Risk evaluation and warning threshold of unstable slope using tilting sensor array

Lin Wang[1] · Ichiro Seko[1] · Makoto Fukuhara[1] · Ikuo Towhata[2] · Taro Uchimura[3] · Shangning Tao[1]

Received: 5 December 2021 / Accepted: 23 April 2022 / Published online: 16 May 2022

Abstract
Slope monitoring and early warning systems are a promising approach toward mitigating landslide-induced disasters. Many large-scale sediment disasters result in the destruction of infrastructure and loss of human life. The mitigation of vulnerability to slope and landslide hazards will benefit significantly from early warning alerts. The authors have been developing monitoring technology that uses a micro-electro-mechanical systems tilt sensor array that detects the precursory movement of vulnerable slopes and informs the issuance of emergency caution and warning alerts. In this regard, the determination of alarm thresholds is very important. Although previous studies have investigated the recording of threshold values by an extensometer which installation of an extensometer at appropriate sites is also difficult. The authors prefer tilt sensors and have proposed a novel threshold for the tilt angle, which was validated in this study. This threshold has an interesting similarity to previously reported viscous models. Additionally, multi-point monitoring has recently emerged and allows for many sensors to be deployed at vulnerable slopes without disregarding the slope's precursory local behavior. With this new technology, the detailed spatial and temporal variation of the behavior of vulnerable slopes can be determined as the displacement proceeds toward failure.

Keywords Early warning · Warning threshold · Disaster mitigation · Slopes failure · Risk evaluation

1 Introduction

Slope instability is a natural hazard that exerts profound influence on the operation and reliability of infrastructure. Unlike engineered structures, natural slopes are not designed for safe performance. As a consequence of natural processes, slopes have heterogeneous material properties. Moreover, slopes are prone to erosion and their gradient changes with time. The underground hydrology is hardly captured in practical engineering. Therefore, quantitatively assessing the extent of slope stability is very difficult in practical situations.

✉ Lin Wang
wang@ckcnet.co.jp

Extended author information available on the last page of the article

Although the movement of landslide mass, which has been considered to be slow in conventional studies, is already a major threat to human activities, rapid and unpredictable slope failure triggered by gravity or heavy rain is more hazardous because it may instantaneously result in enormous loss of human life and the destruction of infrastructure. However, predicting the abrupt failure of slopes to avoid damage is still difficult. Communities in mountain regions are particularly prone to this type of damage. The situation is more serious for transportation infrastructure because its function can be entirely disrupted by a single slope failure (Lee et al. 2013; Sartori et al. 2003). Ongoing global climate change increases the likelihood of heavy and concentrated rainfall, which results in more rainfall-induced slope failures.

As stated above, the mitigation of landslide disasters is difficult and the available funding for conducting elaborate site investigations is far too little. Practitioners have been trying to improve safety by developing slope monitoring and early warning system (EWS) technologies with the objective of predicting slope failure in advance based on the observed slope behavior, and mitigating the extent of damage (Medina et al. 2008). The United Nations International Strategy for Disaster Reduction (UN-ISDR) advocates that EWS should "empower individuals and communities threatened by hazards to act within sufficient time and in an appropriate manner to reduce the possibility of personal injury, loss of life, and damage to property and the environment" (from the UN-ISDR web site, 2006).

Slope monitoring has a long history of practice for landslides that move slowly over months or years until final failure and produce head scarps and cracks in the meantime. Through its extensive application, slope monitoring has become capable of defining the range of moving soil mass. The extensometer, which is installed across well-defined cracks and other displacement discontinuities, is extensively used for monitoring slow-displacement slopes. Saito et al. (1965) and Fukuzono et al. (1985) have proposed an important method for predicting the time of slope failure. Recently, the idea of displacement monitoring using GPS, LIDAR, and InSAR has been introduced (Casagli et al. 2010; Kayen et al. 2006; Yin et al. 2010). The authors' opinion on these technologies is that the high cost of the extensometer may prevent its use when funding is insufficient. Additionally, the above-mentioned technologies may not be able to achieve the required accuracy when very small slope displacement plays a major role in the issuance of warnings. The latter concern will be discussed later in this paper.

Slope movement may occur faster, and only a few days or even hours may elapse until failure. This is particularly the case with rainfall-induced landslides on which the authors are focusing. The limited time preceding the failure makes the use of LIDAR and InSAR very difficult. The displacement of slopes receiving heavy rain is very small and has limited size before failure. Therefore, GPS and InSAR cannot capture the movement. Moreover, the extensometer may not be suitable when the range of instability is unknown and large displacement occurs suddenly, as is the case of rainfall-induced landslides. Because of these problems, the authors (Uchimura et al. 2015) have proposed a different slope monitoring and early warning approach, which is also the subject of this paper.

Many early warning applications employ rainfall thresholds for the issuance of warnings when the monitored rainfall exceeds a predetermined level (Endo 1969; Onodera et al. 1974; Campbell 1975; Caine 1980; Terlien 1998; Nakai et al. 2007; Baum and Godt 2010; Brunetti et al. 2010; Osanai et al. 2010; Nolasco-Javier 2015; Piciullo et al. 2017; Segoni et al. 2018). Because rainfall is widely monitored by meteorological institutions and many private sectors, it is very easy to implement rainfall thresholds. Notably, slope instability is not only affected by the regional rainfall intensity, but also by local soil conditions, the

slope gradient, and geohydrology. Furthermore, the rainfall intensity varies from place to place under the influence of topography. These essential issues are not considered in existing rainfall warning thresholds. Because of these disadvantages, the authors propose a different monitoring approach, which is discussed in this paper.

With regard to early warning, it is of particular importance to ensure a correct alert threshold defined on the basis of a validated predictive model. To accurately issue a slope failure warning, investigations of slope geomorphology, stress–strain behavior of materials, and changes in boundary conditions are required, especially in the case of important works such as dams, highways, etc. However, some or all the investigations above items cannot be carried out for many monitoring projects due to budgetary restrictions. Our research seeks the simplest and most effective method possible. It has become clear that the deformation of the slope surface is the most important phenomenon after experiencing various cases of slope failure.

The selection of the threshold parameter is strictly related to the type of monitoring system and a detailed investigation is required for each system. Particularly, because the field situation changes with time, an innovative monitoring tool should be able to achieve a high frequency of data sampling with automatic and remotely controlled procedures. This feature represents a significant advantage over traditional devices. Moreover, failure prediction receives significant benefits from high-frequency sampling, whereby the ongoing phenomenon is more accurately monitored (Carlà et al. 2017; Segalini et al. 2018).

2 The threshold for early warning of landslides and slope failures

2.1 Model of creep rupture and life prediction

Figures 1 and 2 show the concept of the creep-rupture curve, which exhibits a relationship between the strain caused by creep and time for almost solid material. This diagram classifies the entire process into three stages, which are the primary stage wherein the strain rate decreases with time, the second stage wherein the strain rate is kept constant, and the tertiary phase wherein the creep rate quickly increases until the final failure. The tertiary

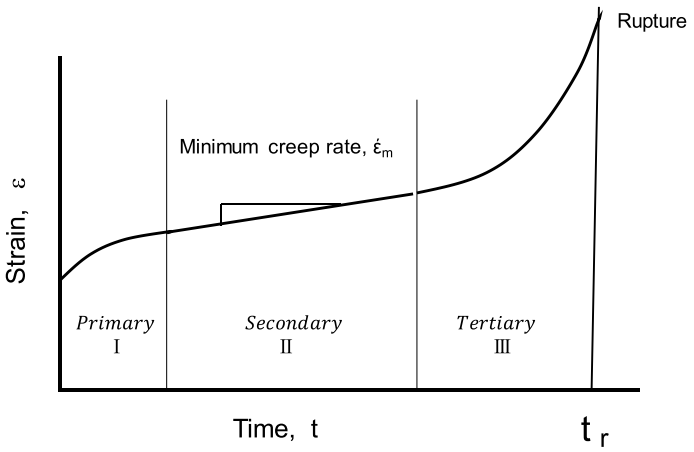

Fig. 1 Conceptual sketch of relationship between strain and time remaining until failure

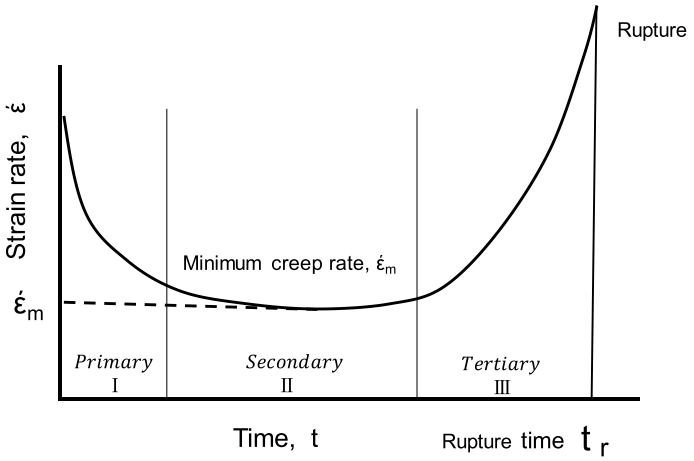

Fig. 2 Conceptual sketch of creep rate changing with time toward failure

phase of this diagram shows that, as time passes, the creep rate increases while the time until failure decreases. The change of the strain rate with time is schematically shown in Fig. 2. The material behavior shown in Fig. 3 is called the Monkman–Grant relationship (1956) and may be useful in predicting the remaining lifetime (time until failure, tr) from the observed creep deformation rate, dε/dt.

$$\log_{10} t_r + m \log_{10} \left(\frac{d\varepsilon}{dt} \right)_{\text{minimum}} = C \tag{1}$$

here tr = time until failure, while m and C are constants.

Figure 3 illustrates the idea of this relationship.

2.2 Saito model for forecasting the time of occurrence of a slope failure

Slopes often develop pre-failure deformation and open cracks before the final large displacement. This does not always mean that the slope will fail, nor does it mean that hazard exists for the traffic close to the slope, even though the movement may continue

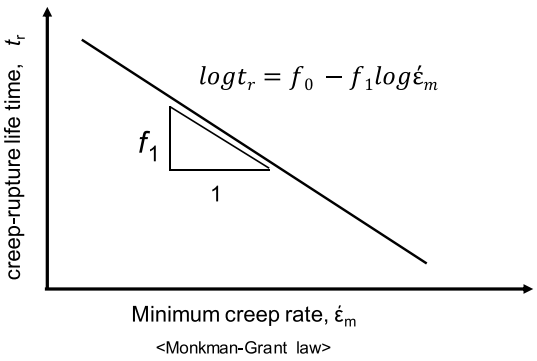

Fig. 3 Relationship between creep time remaining until failure and a minimum rate of creep strain based on Monkman–Grant relationship (Monkman–Grant relationship 1956)

to increase. Thus, it is essential to assess the likelihood of slope failure and the time that remains until failure. In this regard, Saito and Uezawa (1961) monitored the movement of stakes to investigate the possibility of rapid movement before failure and elucidate the creep-rupture behavior of earth slopes. Based on 80 field observations, they found that strain monitoring along the slope surface is the most promising approach for forecasting the time of slope failure. Their study was extended to laboratory soil tests wherein the creep-rupture process of soil was investigated. One of their most important findings was that the time until failure is inversely proportional to the constant strain rate in the secondary creep phase (Fig. 2). This relationship is independent of the soil type and testing method, and is universally valid for all tested materials. Moreover, this relationship was extended to the tertiary phase of creep, and a method for predicting the time of slope failure was proposed. Hence, this allows for an approximate prediction based on the constant strain rate in the secondary phase of creep, and for more precise estimation using the strain rate in the tertiary creep range. Figure 4 presents the results obtained from 34 laboratory tests using various soils. Notably, the results are similar to the implications of the Monkman–Grant relationship (Eq. 1). Saito and Uezawa (1961) fitted Eq. 1 to the test results and explicitly established Eq. 2, as follows:

$$\log_{10} t_r = 2.33 - 0.916 \log_{10} \left(\frac{d\varepsilon}{dt} \right)_{\text{minimum}} \pm 0.59 \tag{2}$$

where *tr* is expressed in terms of minutes and the strain is expressed in terms of 10^{-4} per minute, respectively. From Fig. 4, this formula is independent of the soil type and the testing methods. The range of data scattering in this Fig. is ± 0.59 and contains 95% of the data points. This extent of scattering was assessed to be appropriate for soil (Saito et al. 1961). The creep law is not used assuming that failure is caused by deviatoric creep.

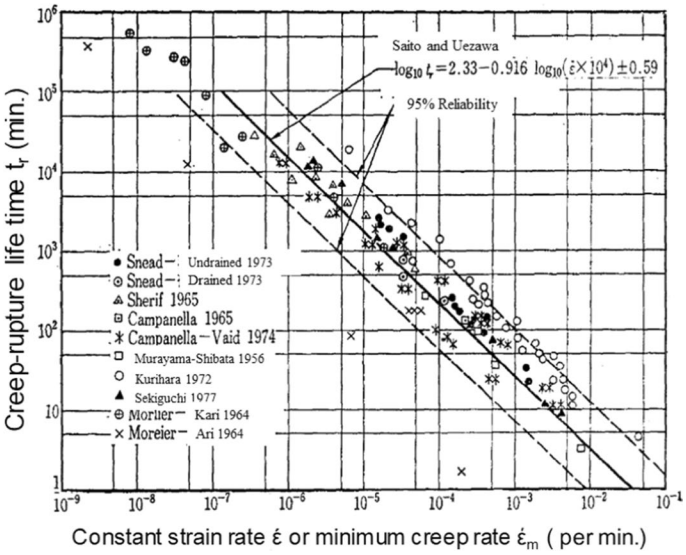

Fig. 4 Relationship between creep time remaining until failure and strain rate or minimum creep rate based on results of geomaterial testing (Saito and Uezawa 1961)

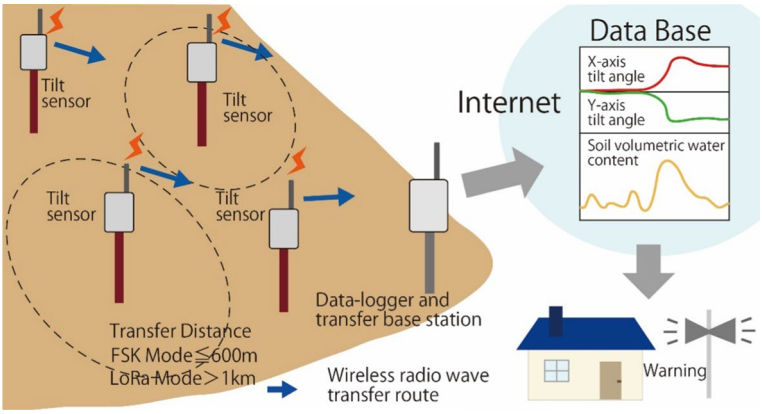

Fig. 5 Early warning of slope failure using multi-point sensing of tilt and volumetric water content

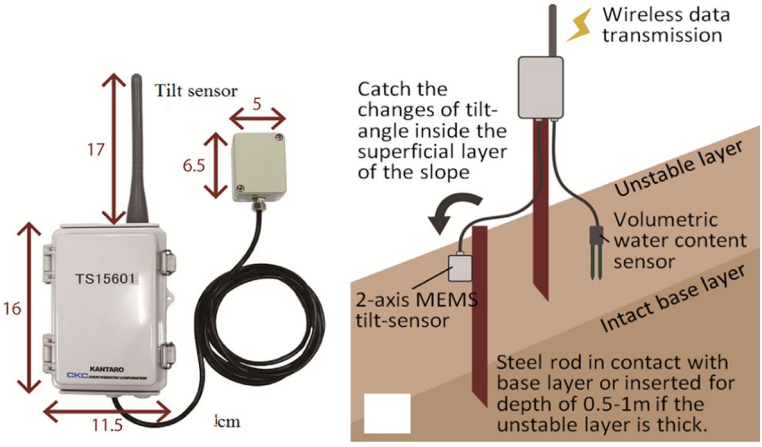

Fig. 6 Schematic illustration of MEMS tilt sensor for early warning (volumetric water content sensor is optional)

2.3 MEMS tilt sensor for monitoring of vulnerable slopes

The authors have been developing a new type of slope monitoring device with the objective of predicting the time of failure triggered by heavy rainfall (Uchimura et al. 2015). The major issue in the development of this technology is the use of micro-electro-mechanical systems (MEMS) sensor for the tilting angle, which is attached on the top of a steel rod embedded in a slope (Figs. 5 and 6) and precisely measures the inclination (rotation) angle of the rod when it is pushed laterally by the slope's moving surface soil. Because rainfall-induced slope failure occurs within several hours after a precipitation event, where there is no pre-existing deformation or cracks, the traditional methods of the extensometer, LIDAR, and so on, are not helpful. Because MEMS sensors are less expensive, many sensors can be deployed over the investigated slope. The monitoring data are sent to the office through a wireless network and interpreted. To date, MEMS tilt sensors have been deployed at more than 100 sites, both domestically and internationally (Japan, Australia, China, Taiwan, and

a few more countries). The threshold for issuing an early warning is specified as the rate of inclination equal to 0.1°/hour (Uchimura et al. 2015).

3 Validation of tilt sensor for slope monitoring

Previously, MEMS tilt sensors have been used at more than 100 sites with slope instability. Most of these slopes did not fail, but several of these slopes have failed with and without rainfall and provided important data. Based on these data, the warning threshold has been determined as 0.1°/hour. In this section, various cases that have not been reported are discussed.

3.1 Prevention of secondary disaster during restoration of failed slope–Fukuoka pref., Japan

An EWS was successfully used in 2015 in Fukuoka Prefecture, Japan. When this region received heavy rainfall during typhoon No. 11 "Nangka" on July 17 and 18, the slope collapsed and the local road was closed to traffic (Fig. 7). This slope comprises Funi volcanic rock of andesite karst, tuff breccia, and tuff. To safely keep one lane open for traffic during slope restoration, the slope movement was monitored by a set of tilt sensors as shown in Fig. 7. The traffic was intended to stop if the tilt sensor detected an excessive tilting rate during the slope restoration works.

Figure 8 shows the plot of the tilt angle and the rainfall data on July 21st and 22nd, shortly after the main slope collapse. The slope was considered to be prone to further failures during the restoration works. From 4 to 8 PM on July 21st, that is, immediately after the tilt sensor installation, the tilting rate of 0.083°/hour was recorded and continued until 8 AM on July 22nd. Thereafter, the tilting rate accelerated to 0.89°/hour, possibly owing to rainfall amounting to approximately 10 mm from 8 to 9 AM. Furthermore, owing to further rainfall after 11 AM, the tilting rate sharply increased to 12°/hour after 12 PM and the slope finally collapsed at 12:30 PM. Thus, the field monitoring helped control the traffic during the critical period and ensured the safety of human life.

Uchimura et al. (2015) summarized the tilting rates monitored at several natural slopes subjected to heavy rainfall. Figure 9 shows the sets of the tilting rate and time remaining until failure. This data group is placed in the right half of the Fig. under the indication "large deformation" or "failure". Another group of data was obtained from cases wherein the tilting rate was small and the movement was stabilized without failure (see "stabilization" group). Figure 10 shows the detailed definitions of the tilting rate and time, where T_i is the time until failure or stabilization, and R_i is the tilting rate. When the slope failed, "time" means the time that elapsed from measurement until failure. Conversely, when failure did not occur, "time" means the time between measurement and stabilization.

Based on practical experience at many sites with and without failure, Fig. 9 presents information over a wide tilting rate range from 0.0001°/h to 10°/h. Obviously, a higher tilting rate is associated with less time until failure, which suggests that urgent evacuation is required. When the tilting rate exceeds 0.1°/h, the time remaining until failure is one hour at minimum. Therefore, the authors (2015) recommend that a warning and evacuation order should be issued at this tilting rate. Moreover, precaution may be issued at a tilting rate of 0.01°/h to ensure safety, because the time left until failure will be several hours or longer.

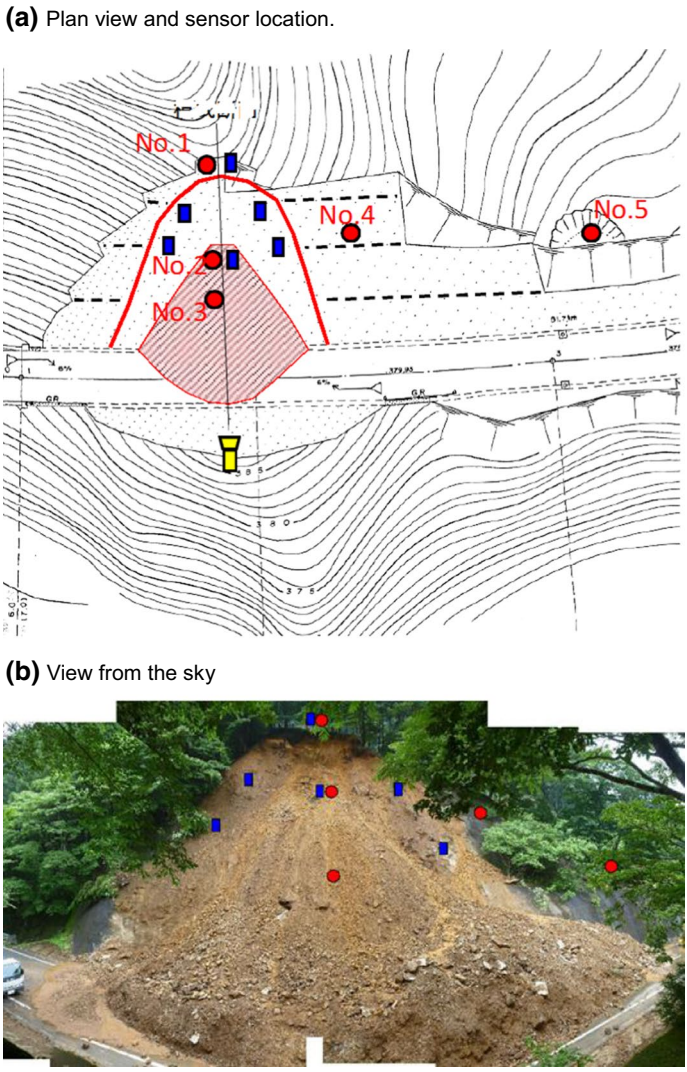

Fig. 7 Monitored slope in Fukuoka

In the typical case wherein the surface soil thickness is 150 cm (Fig. 6), the 0.01°/hour and 0.1°/hour tilting rates correspond to the displacement rates of 150 × tan (0.01°) or 150 × tan (0.1°), that is, 0.026 cm/hour or 0.26 cm/hour, respectively. Hence, it is extremely difficult for GPS, LIDAR, and InSAR to continuously monitor this small movement during heavy rainfall. Therefore, the authors prefer using tilt sensors. The following sections discuss the practical experience acquired at other slope-monitoring sites and used to validate the warning principle described above.

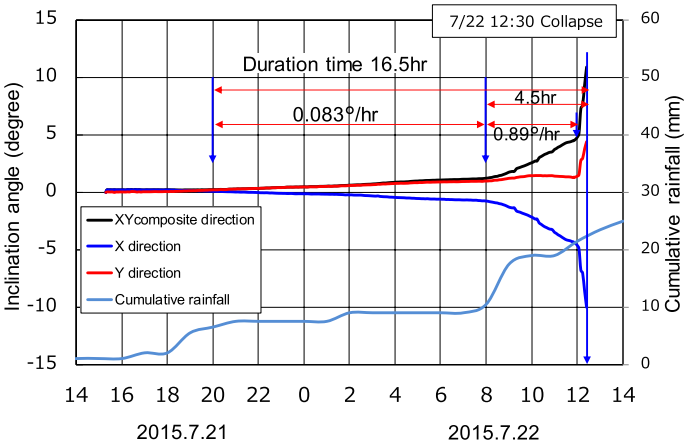

Fig. 8 Time histories of monitored data at Fukuoka site

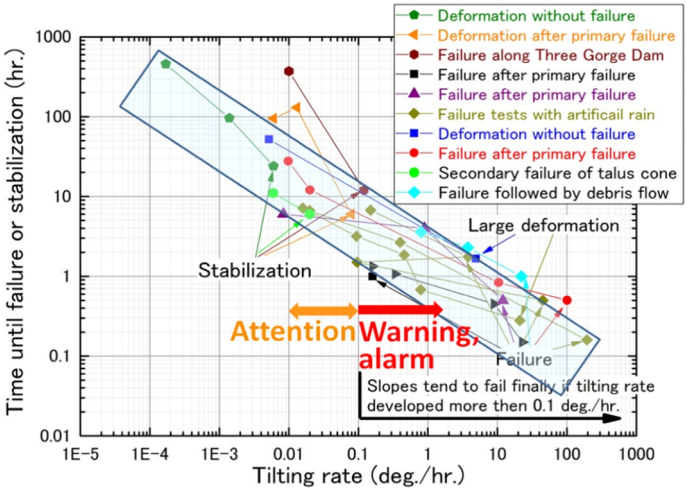

Fig. 9 Tilting rate varies with time until slope failure or time of stabilization (summary of several case histories)

Fig.10 Definition of tilting rate and time remaining until failure

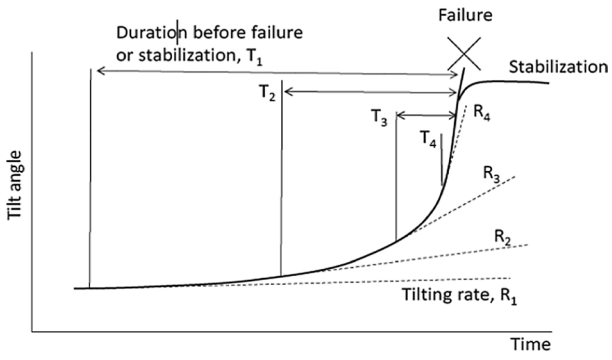

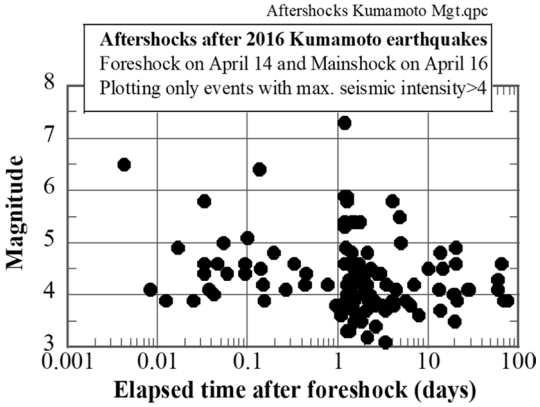

Fig. 11 History of aftershocks following the 2016 Kumamoto earthquakes

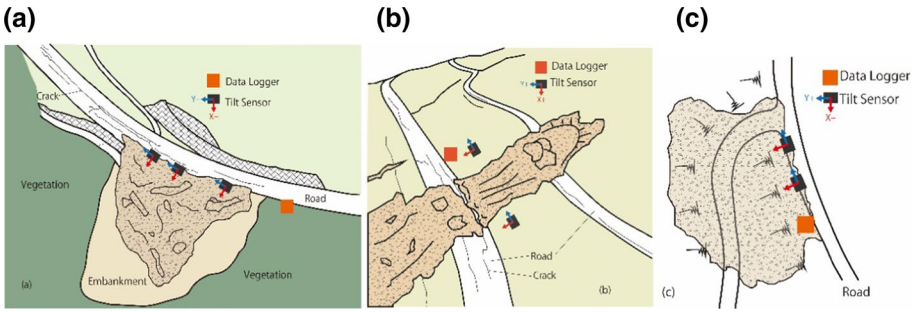

Fig. 12 Location of tilt sensors used for early warning at three slope disaster sites after the 2016 Kumamoto earthquakes

3.2 Experience with the tilt sensor monitoring in Kumamoto Prefecture, Japan

Kumamoto in Kyushu Island, Japan, was hit by an earthquake swarm in April, 2016. Among the quakes, the top two events had a moment magnitude (Mw) of 6.2 on April 14th and Mw = 7.0 on April 16th. Because the focal depth of these earthquakes was shallow (11–12 km) and immediately below human communities, many houses were destroyed and 273 people were killed. These seismic events induced slope failure at more than 190 sites and urgent restoration was required. Because this was a seismic swarm, many aftershocks occurred for months after the major shocks (Fig. 11). Therefore, it was crucial to protect the people living close to unstable slopes. This situation led to the implementation of EWS that recorded tilt angles, water content in the soil, and rainfall intensity. Figure 12 shows three slope monitoring sites that were located in Nishihara Village, to the west of the Aso volcanic caldera in Kumamoto Prefecture. The objective of monitoring was to avoid further disaster when the road reconstruction works were in progress.

At two of the monitored sites, slope failure occurred in the early morning of June 20–21, 2016, in the course of ten hours of precipitation amounting to 200 mm (Fig. 13). At site (a), a small slope failure occurred at the position of the wireless sensor unit K-2 (Fig. 12a) during a precipitation event on June 21, 2016. At this site, two additional wireless sensor units maintained normal operation. After the monitoring system detected abnormal

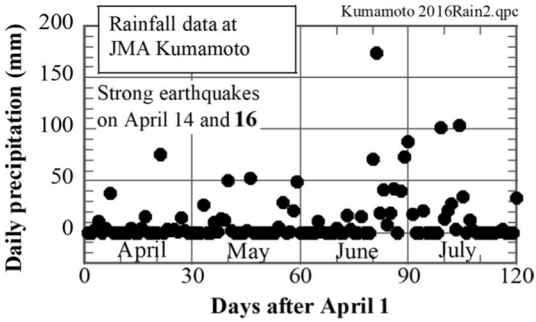

Fig. 13 Precipitation per day at JMA station in Kumamoto

behavior through the wireless sensor (Fig. 14), a caution alert and subsequently a warning alert was automatically issued. Eventually, the slope failed.

Figure 15 shows the data at the site (c) where another slope failure occurred. The inclination of the tilt sensor K-5 started to change quickly at around 02:00 o'clock on June 21st when the peak rainfall intensity had finished. As can be seen, the tilt angles in the X and Y directions underwent notable changes. The recorded rate of the tilting angle exceeded the threshold (> 0.1 degree/hour) and a warning was issued before the slope failure. Because a warning could be issued before the monitored slope failed, based on the data obtained from the sensors, it is reasonable to say that the proposed monitoring method can provide valid information with regard to instability during rainfall that occurs after the slopes have been disrupted by seismic activity.

3.3 Practical tilt sensor monitoring in Tokyo

Because of the heavy rain associated with Typhoon No. 21 "Jebi" on October 23, 2018, a part of industrial waste landfill collapsed. Consequently, a part of the collapsed sediment flowed and reached the prefectural road below the slope (Fig. 16). Accordingly, a temporary protective fence and large sandbags were placed along the road, but drastic

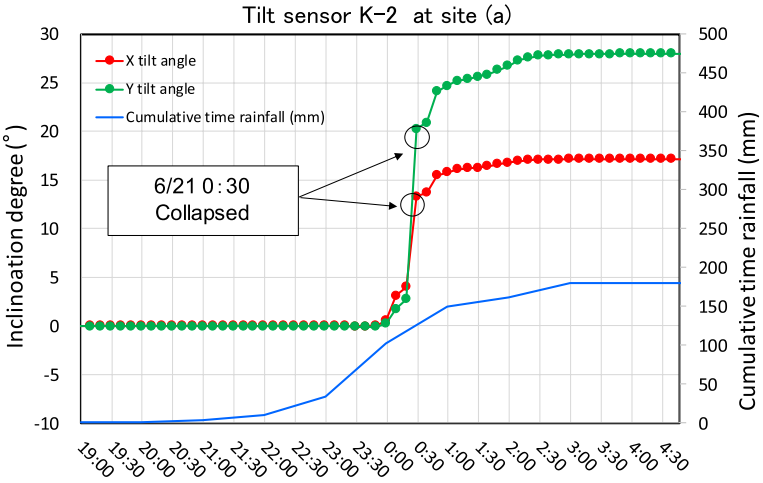

Fig. 14 Tilting and rainfall records at monitoring site (a) in Kumamoto (June 20–21, 2016)

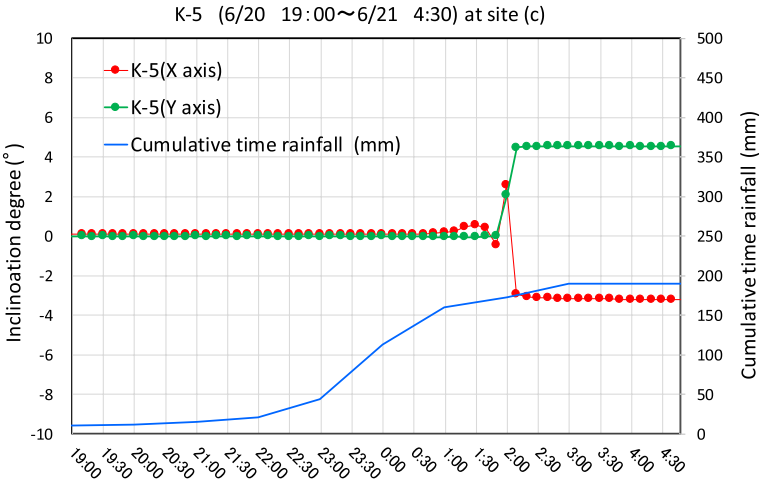

Fig. 15 Tilting and rainfall records at monitoring site (c) in Kumamoto (June 20–21, 2016)

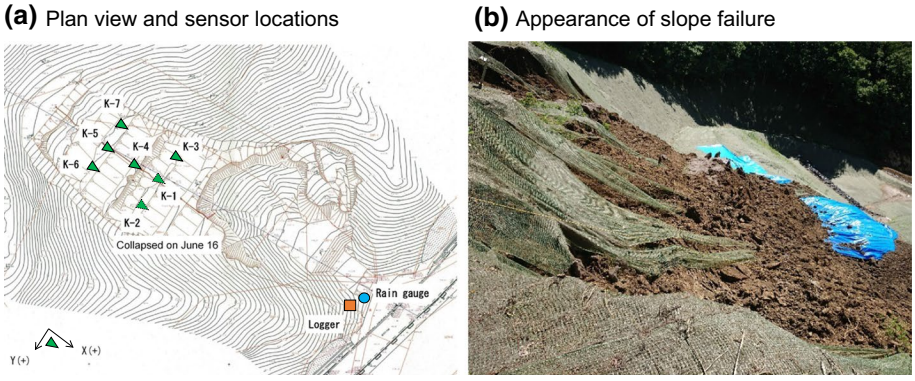

Fig. 16 Monitoring at landfill slope in Tokyo

measures against the landfill collapse were not implemented. However, it was highly likely that slope failure would reoccur during the rainy season in 2019. Hence, the Environment Bureau of the Tokyo Metropolitan Government installed three extensometers at the edge of the landfill for monitoring. Moreover, three tilt sensors were installed for research purposes.

Figure 17 shows the monitored time history of the cumulative rainfall and the tilt angles. When the rainfall, which cumulatively amounted to 38 mm, occurred before 8 PM on June 15, there was no significant change in the records of tilt sensors K-1 and K-2. Thus, the situation remained relatively stable. A few hours later, in the early morning of June 16, the tilt angles started to increase toward infinity at 5:10 AM (slope collapse). The tilting rate of K-1 reached 0.58°/hour (X-axis of slope direction) at 4 AM on June 16, and K-2 reached 0.20°/hour (X-axis of slope direction) at 3:30 AM on the same day. Because the record of the tiltmeters accumulated in the negative direction of the X-axis (toward the top of the slope), it is believed that the slope failure mechanism was associated with circular slip (rotation).

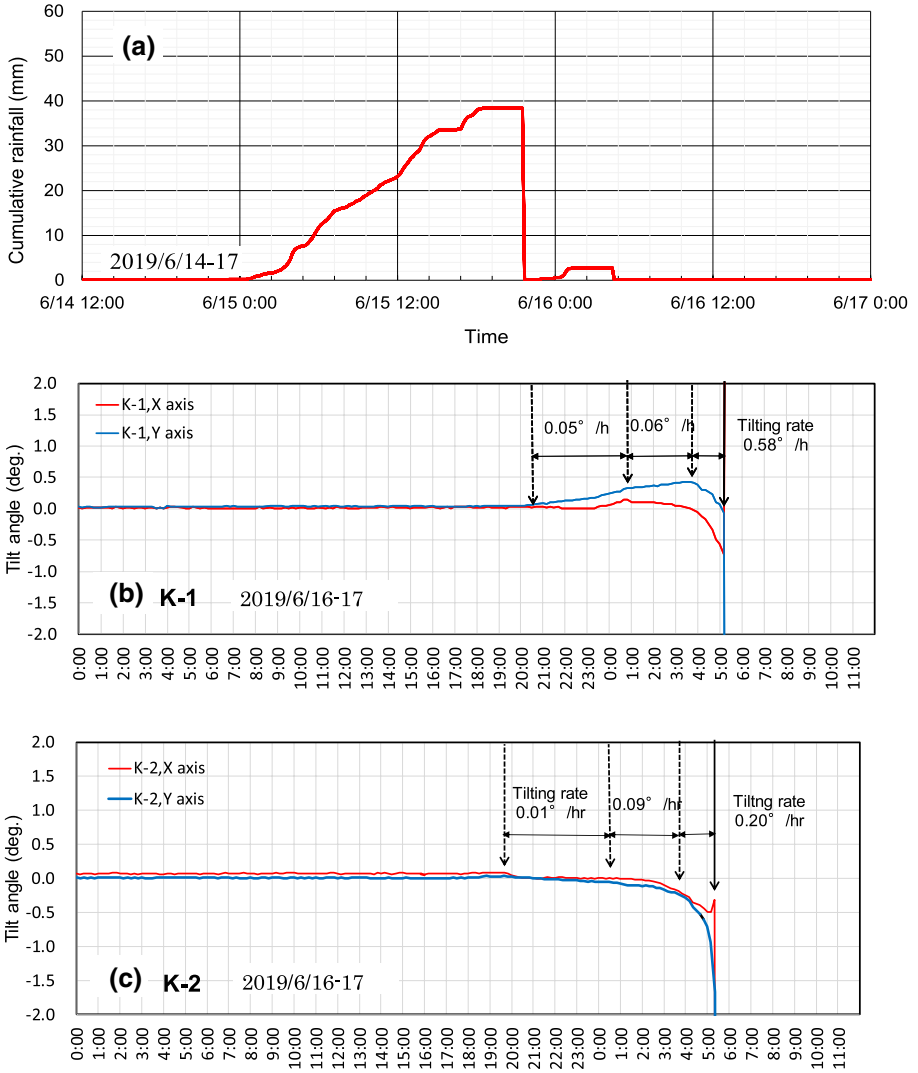

Fig. 17 Recorded cumulative rainfall and tilt angles at sensor K-1 and K-2 at the site shown in Fig. 16 (June 15th and 16th)

3.4 Landslide monitoring at three gorges dam site, China

In 2008, the same monitoring system was installed on a slope along the Three Gorges Dam Reservoir in China. This site, Sai-Wan-Ba area, is located on the right bank of the reservoir, near Wanzhou Ward, 80 km eastward of Chongqing City (Fig. 18). After the impounding of the reservoir, several landslides were initiated, as had been predicted by geological investigations (Fig. 19). Three sensor units were placed on appropriate slopes with consideration to the location and site of the landslide mass. Figure 20 illustrates the cross-section of the unstable slope including the position of "sensor unit 2". The slope mainly consists

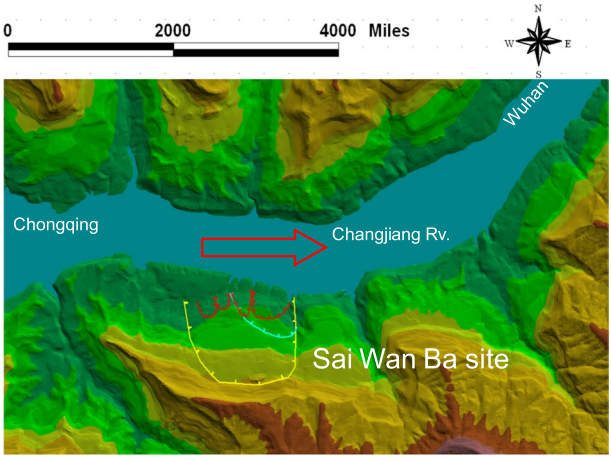

Fig. 18 Location of Sai Wan Ba landslide site

Fig. 19 New landslide on June 7, 2009, at Sai Wan Ba

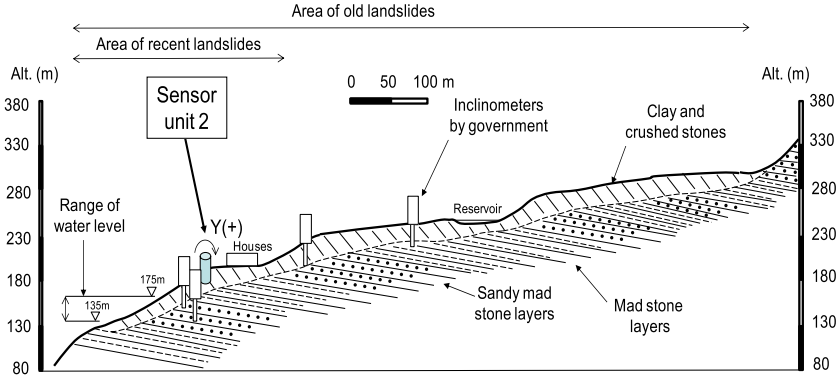

Fig. 20 Cross-sectional view of Sai Wan Ba landslide site passing position of the sensor unit 2

of mudstone or sandy mudstone layers. The slope surface is covered by a deposit of clayey soil with some crushed mudstone with an average thickness of 15 m. The recent landslide body has a length of approximately 350 m and a slope angle of 5–15°. The dam has been in service since 2008, and 30 m of periodical changes in the water level of the reservoir (Changjiang River) are scheduled every year for effective dam operation. Moreover, the site is located in a subtropical region, where heavy precipitation events occur, and some displacement on the slope surface was reported in the summer of 2008.

The slope monitoring resumed in October 2008. Heavy rainfall that occurred on June 7 and 8, 2009, caused significant displacements in the monitored landslide bodies including the position of the sensor unit 2. The time history of the tilting angles of the pole in the X and Y directions is shown in Fig. 21. During rainfall events, the tilting angles gradually increased, and the tilting angle in the Y-axis reached 5° at the beginning of June 2009. The positive values of the tilting angle in the Y direction mean that the pole tilted toward the top of the slope. In contrast, the X component of the tilting angle that was oriented in the lateral direction of the slope had relatively smaller values. During this event, the rate of the Y tilting angle was 0.125°/h, while the rate just before this event was approximately 0.008°/h. This quick behavioral change was induced by the ongoing landslide.

3.5 Landslide monitoring at Zhongpu Township, Chiayi County, Taiwan

As an advanced version of tilt angle monitoring, multi-point monitoring units were installed at a landslide site in Zhongpu, Chiayi County, Taiwan, in June 2017. The multi-point monitoring system can deploy and synchronize 30 or more tilt sensors such that the distributed displacement (tilting angle) of the considered slope may be monitored. Another advantage is that a large number of sensors is less likely to overlook local instability in a slope. The monitoring slope is close to the national route No.135–2 and shows typical landslide phenomena. Additionally, the slope moves in a gradual manner after rainfall. Figure 22 illustrates the overall view of the slope dipping from the bottom right of the photo toward the left. The slope comprises shale and sandstone shale interbedded by shaly sandstone and limestone, and slides along an established geological joint direction.

To investigate the depression of the road and the slope's possible sliding mechanism, a field survey was conducted for the local geology and hydrological environment by monitoring the slope movement using tilt sensors, a borehole inclinometer, and water

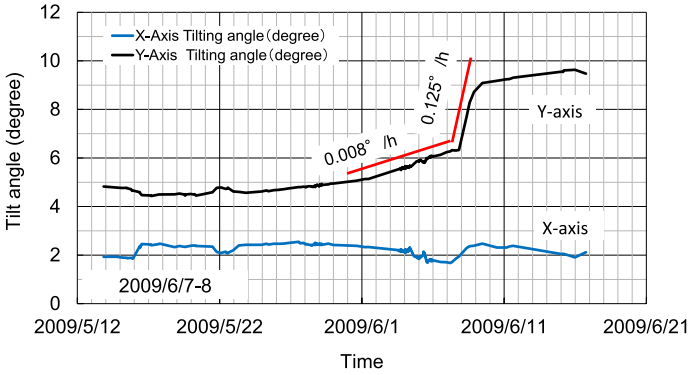

Fig. 21 Time histories of tilting angle obtained by sensor unit 2 at Sai Wan Ba

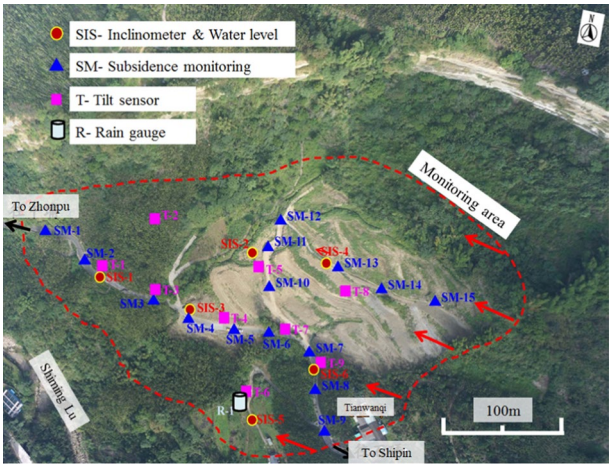

Fig. 22 Location of tilt sensors on moving slope of national route No.135–2 in Taiwan

level measurement starting from June 2017. Specifically, multi-point measurement was the primary activity at this site, as shown in Fig. 22. Nine tilt sensors were installed to adequately cover the moving soil mass, and the tilt angle was measured every 10 min. The monitoring data were collected by a server on the opposite side of the valley and were sent out to the office through the internet.

The pavement cracks and translation of the retaining wall along the national route No.135–2 are shown in Fig. 23. The traffic was stopped when these problems were detected. Figure 24 presents the results of the combined XY inclination value and daily rainfall at tilt sensor T9 located at the top of the slope, which is close to the retaining wall where many cracks and lateral displacement were detected. It is still unclear why the tilting angle shown in Fig. 24(a) remarkably increased in the middle of August and September, and after the end of October when the local rainfall was negligible. The possible reason for this is that the underground hydrology delayed the rainfall effects, but this was not confirmed. Notably, Fig. 24 shows that slopes may start to move regardless of the antecedent rainfall.

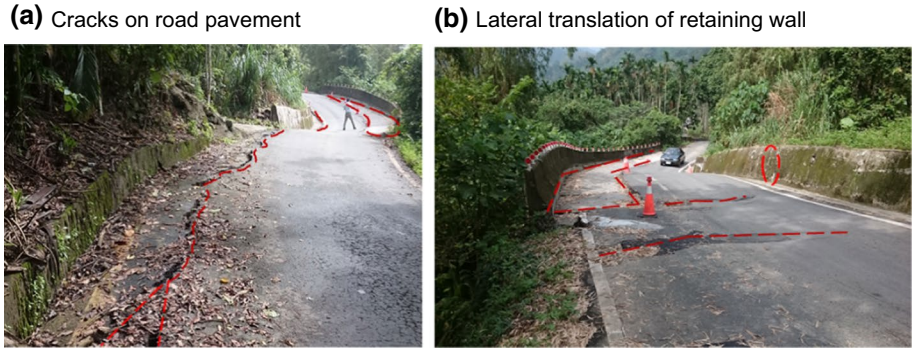

Fig. 23 Cracks in the road surface and lateral translation of retaining wall on side of national route No.135–2 in Taiwan

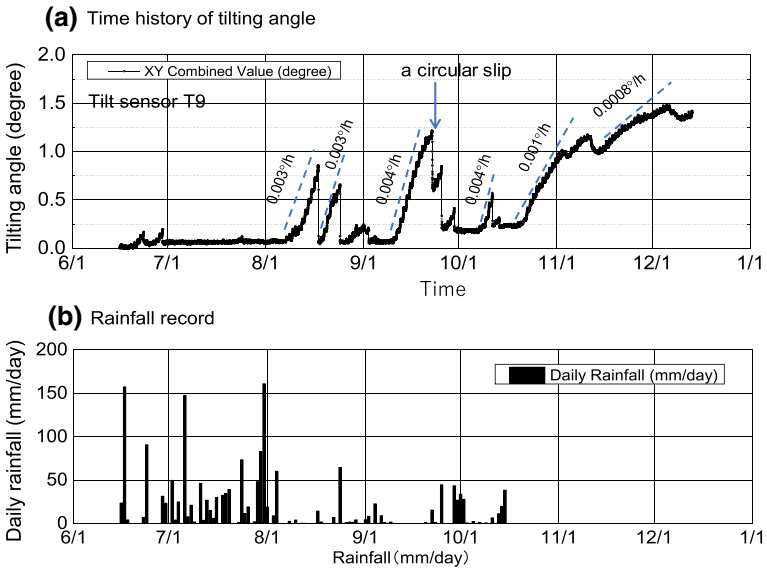

Fig. 24 Inclination value and daily rainfall of tilt sensor T9 on top of Zhongpu slope site close to national route No.135–2 in Taiwan

One of the advantages of multi-point monitoring is the three-dimensional view of the slope deformation, which is shown in terms of the distribution of the sensors' tilt angle in the slope gradient direction (Fig. 25). Throughout the monitoring period of six months, the head (Sensor T-9) and bottom (Sensor T-1) of the slope exhibited a larger inclination toward the bottom of the slope, while substantial tilting was observed in the opposite direction (toward the top of the slope) in the middle part (Sensor T-4). This feature was also observed in other slopes, as will be discussed later, and maybe an interesting feature of slope instability. Hence, it is thought that slope failure was unlikely because the cumulative tilt angles (0.201° at T-2, −0.394° at T-4, and 0.082° at T-9) did not exceed 1°. Moreover, at all sites, the tilting rate did not exceed the 0.01°/h threshold for issuing a caution alert. Thus, the failure of this slope was unlikely, but the slope movement did not stop and the monitoring had to continue.

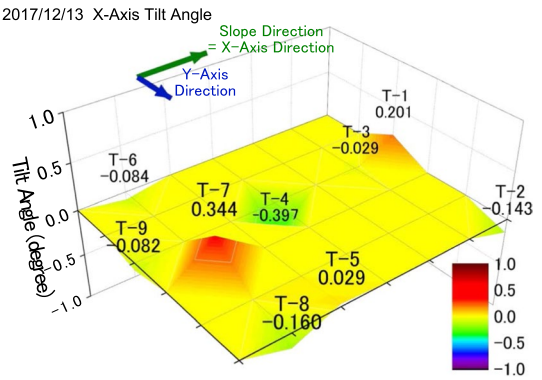

Fig. 25 Distribution of tilt angle at X-axis (slope) direction close to national route No.135–2 in Taiwan **a** Sensor locations at the slope in Queensland, Australia (X denotes downslope direction) **b** Cross-section from GPR profile showing the position of white clay/bedrock reflector (dashed line)

3.6 Detection of rain-induced landslides in critical slopes in Lake Baroon Catchment, Maleny Plateau, Brisbane, Australia

The Landers Shute Water Treatment Plant (LSWTP), sourced from the Baroon Pocket Dam (BPD), supplies the Sunshine Coast with 50–120 ML/day of water. This Dam is vital for potable water production in South East Queensland. Additionally, SEQWater has committed to a potential 300-year lifespan for the Dam. Moreover, SEQWater considers steep and unstable slopes as "Extreme Uncontrolled Risks" to the LSWTP. The investigated area is the Lake Baroon catchment in Maleny (Fig. 26), and is located approximately 100 km north of Brisbane (26.76 0S 152.85 0E). The Mapleton-Maleny Plateau, wherein the Lake

(a) Sensor locations at the slope in Queensland, Australia (X denotes downslope direction)

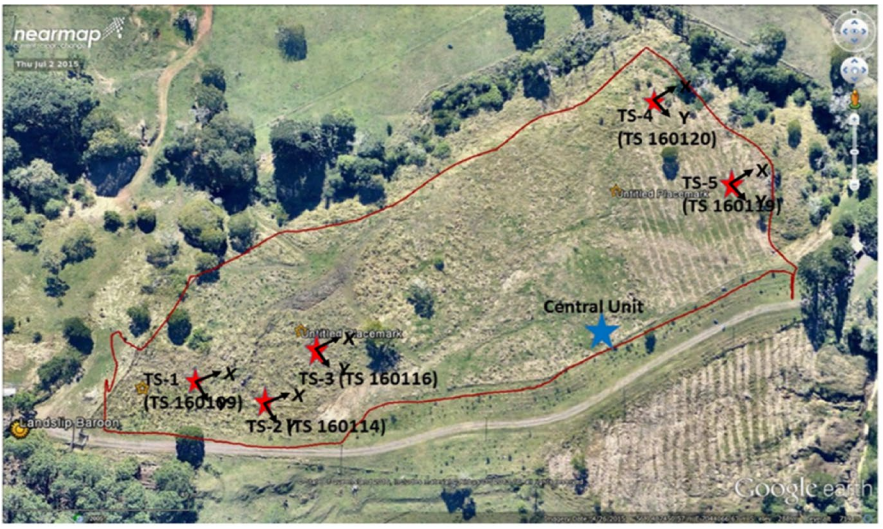

(b) Cross-section from GPR profile showing the position of white clay/bedrock reflector (dashed line)

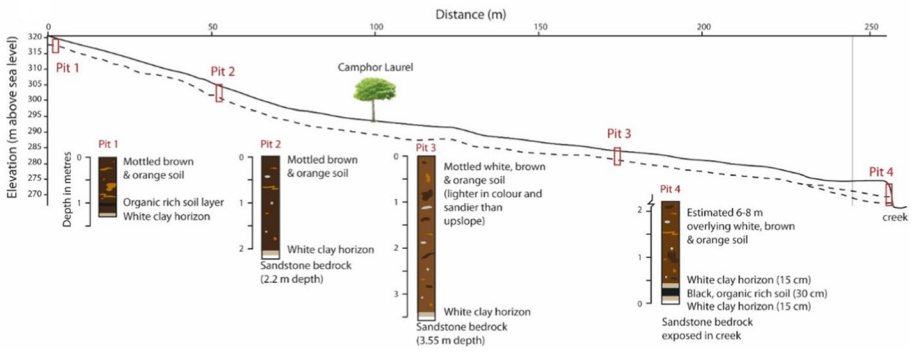

Fig. 26 Site of slope monitoring in Queensland, Australia (Abeykoon et al. 2018, 2019)

Baroon catchment is located, has been documented and discussed since the mid-1950s as an area that is highly susceptible to rainfall-induced slope failure. Additionally, the slope failure and mass movement of sediment into the waterways within the Lake Baroon catchment are recognized as a significant risk to the water quality and water storage capacity of Lake Baroon, which is used to supply water to South East Queensland. Approximately 170 mass movement landforms have been identified within the Baroon catchment, and the investigated area is one such high-risk slope. In 2008, this landslide site hosted a voluminous single-failure rotational landslide after heavy rainfall. The study employed a wide range of data collected from May 10, 2016 to 2020 to predict the slope failure under rainfall infiltration (Abeykoon et al. 2018, 2019).

Slope failures are thought to have various patterns. Various collapse patterns are classified, such as erosion collapse, slope failure, large-scale collapse, landslide collapse, etc. furthermore, slope behavior upon failure depends on slope geomorphology, stress–strain behavior of materials. The soil extracted from the monitoring site was subjected to laboratory tests to determine the required soil properties for the numerical analysis. Table 1 summarizes the results of the laboratory tests conducted to determine the index properties of the soil according to Australian standards (Abeykoon et al. 2018, 2019).

A real-time monitoring system comprising five sensor units (TS1, TS2, TS3, TS4, and TS5) and a central logging station was installed on the slope as shown in Fig. 26. Each sensor unit comprised its own logging and transmission unit, a MEMS tilt sensor, volumetric soil moisture sensor, and temperature sensor.

The two-dimensional distribution of the tilt angles that accumulated during the precipitation events between June 15 and November 10, 2016, is shown in Fig. 27, where the red color indicates that the inclinometer tilted toward the slope bottom, and the blue color indicates the opposite tilting direction. As can be seen, the slope continuously deformed throughout the monitoring period.

The TS1 sensor located at the top of the moving slope tilted (rotated) more than 2° degrees toward the bottom, as shown in Fig. 27(h). The TS2 sensor located outside the moving slope did not move in the early stage of monitoring. However, a minor response was initiated in the later stage (after Fig. 27(e)). This was probably the reactivation of failure in this part, which was caused by the movement of and overloading from the sliding mass above TS2. The TS3 sensor located in the middle of the slope inversely tilted more than 2° toward the top of the slope. The TS5 sensor at the bottom of the landslide tilted again toward the bottom. These findings reveal that the downslope tilting of the sensors was predominant close to the top and bottom of the slope, whereas upward tilting was observed in the middle of the slope. Interestingly, this point is consistent with the findings at the Taiwan site (Fig. 25) and maybe a common feature of slope failure. In other words, tension was predominant in the surface soil close to the top of the slope, and a tilt sensor attached to a rod (Fig. 6) inclined in the downslope direction. The sensor closes to the slope bottom inclined in the same direction probably because it was pushed by the entire

Table 1 Soil index properties at the slope in Queensland, Australia

Classification Test	Results
Grain size	% finer than 75 μm > 79%
Distribution	Clay % = 41.0%
Atterburg Limits	LL = 67.2%, PI = 28.2%
Linear Shrinkage	LS = 13.4%

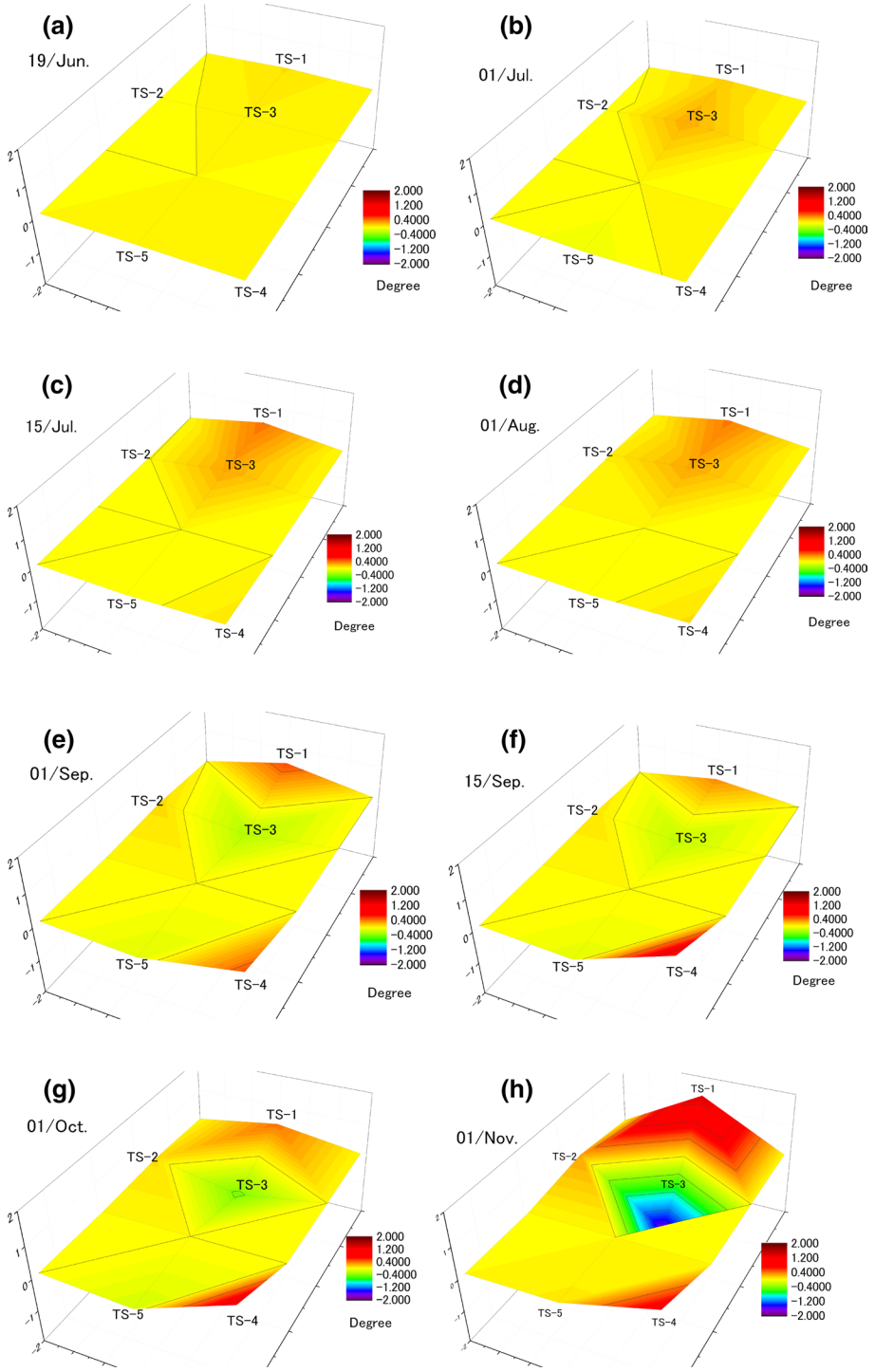

Fig. 27 Distribution of tilt angle that accumulated in 2016 (Queensland, Australia)

mass of the moving slope. In contrast, the sensor in the middle rotated backward, which implies landslide mass rotation along a circular slip plane. By installing an array of multiple sensors, it was possible to investigate the recorded distribution of tilt angles and detect erroneous cases that do not fit the above-mentioned pattern. Thus, a slope monitoring and warning system can avoid false alarms caused by the local fluctuation of data, but this error cannot be avoided when using a single-sensor system.

Figures 28 and 29 compare the changing situation of the slope between October 28, 2017, and February 10, 2018. As can be seen, the slope deformation increased during this four-month interval. This is consistent with the results of tilt angle monitoring, which reveal that the angle increased with time.

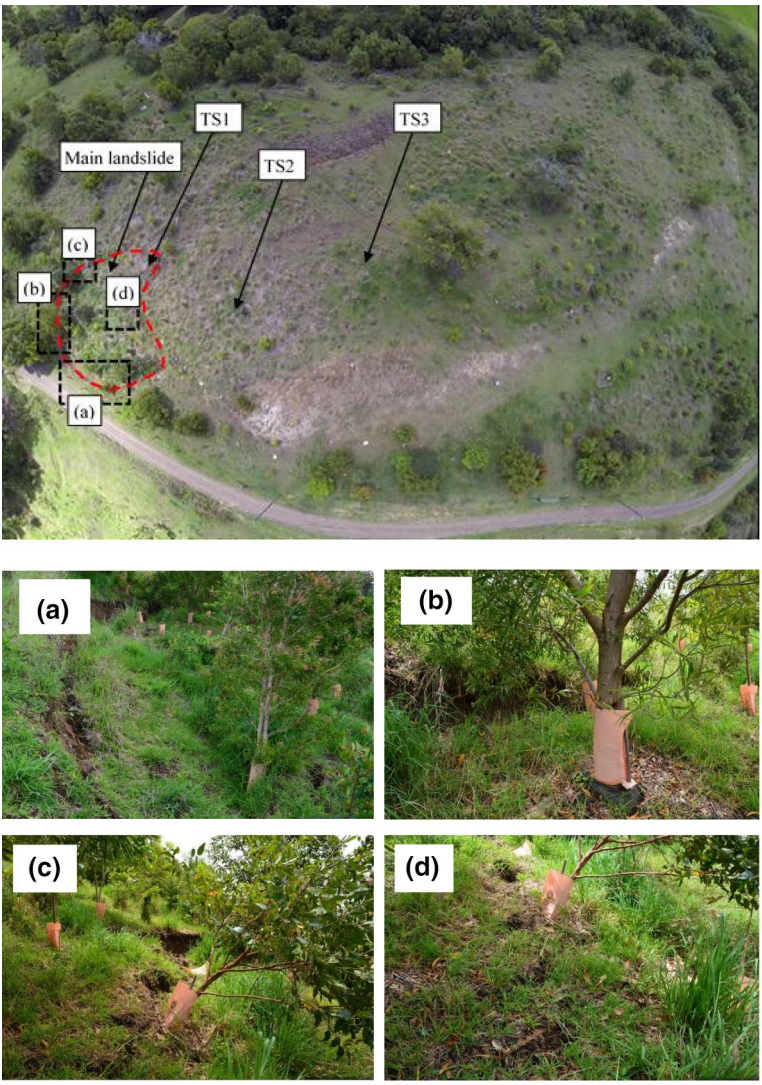

Fig. 28 View of landslide area on October 28, 2017 (Queensland, Australia)

Fig. 29 View of landslide area on February 20, 2018 (Queensland, Australia)

3.7 Slope monitoring at Manzawa, Yamanashi, Japan

The Manzawa site in Yamanashi Prefecture, Japan is situated near national road 52 and includes a large-scale reactivation of an old slope failure featuring rockfall involving the detachment and rapid downward movement of rock. Because traditional slope monitoring methods such as extensometers and borehole inclinometers are considered to be expensive and irrelevant to the three-dimensional monitoring of slope behavior, multi-point monitoring using tilt sensors was attempted.

Figure 30 shows an aerial view of the Manzawa slope and Fig. 31 shows the location of the multi-point tilt sensors. The spacing between the sensors was set to five meters, and 66 sensors were deployed in total. Notably, monitoring was carried out only in the lower part of the slope as shown in Fig. 30, owing to administrative reasons.

The distribution of the accumulated tilt angle over the monitored area is shown in Fig. 32, and its local variation is obvious. The rate of tilting during the respective precipitation events is shown in Fig. 33. The precipitation events on April 20, 2017, June 3, 2017,

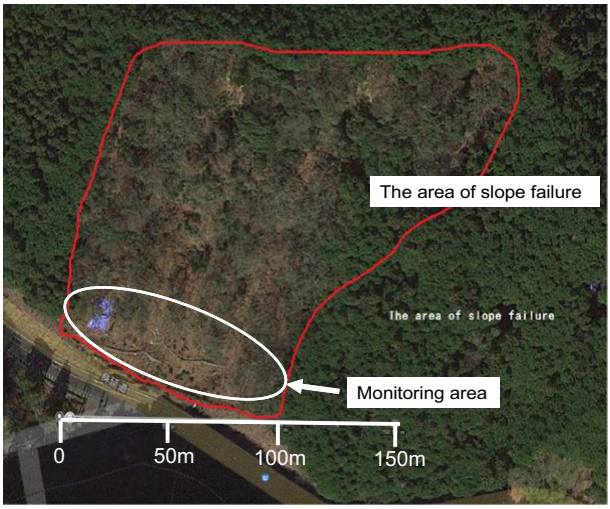

Fig. 30 Area of slope instability at Manzawa site, Japan

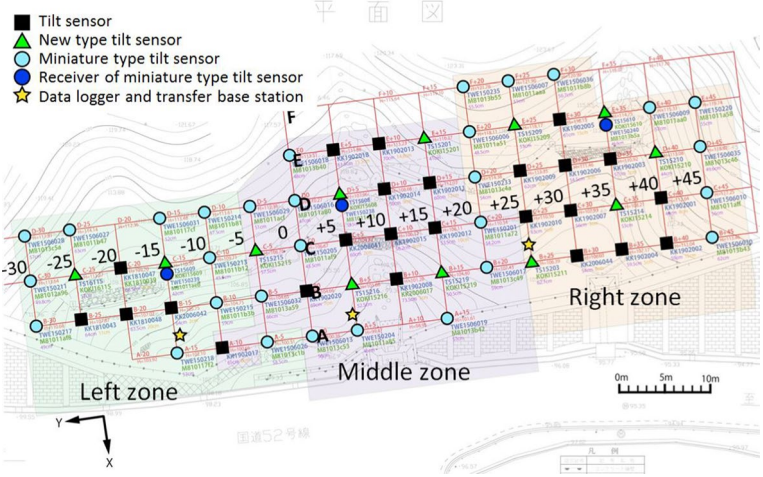

Fig. 31 Multi-point tilt sensor locations at Manzawa site

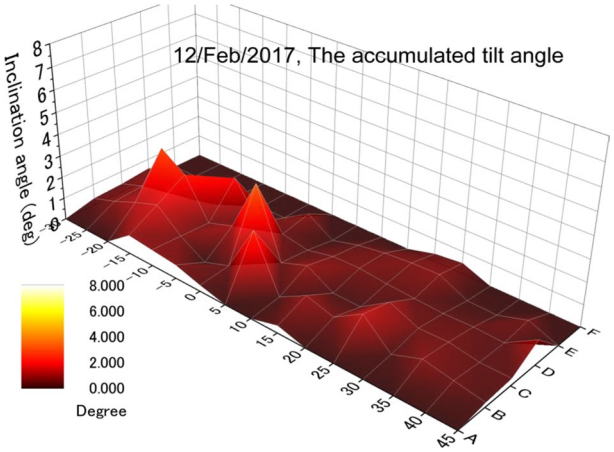

Fig. 32 Distribution of accumulated tilt angle at Manzawa site

and August 13, 2017, caused relatively higher tilting rate values, but these values did not exceed the precaution threshold of 0.01°/hour. Another issue is that a higher tilting rate occurs at different points during different precipitation events, as revealed by comparing the data obtained on April 20 to those obtained on June 3 and August 13. During the two-year field validation, there was no significant change in the tilting angle, and no alert was issued. Thus, the slope was assessed as stable.

4 Assessment of remaining time until slope failure

The EWS does not only make use of tilting sensor array records but also rainfall records. Rainfall warnings of this system were issued based on hourly rainfall, cumulative rainfall, short-term effective rainfall, and long-term effective rainfall. However, the slope did not move even if rainfall warnings were issued in many cases.

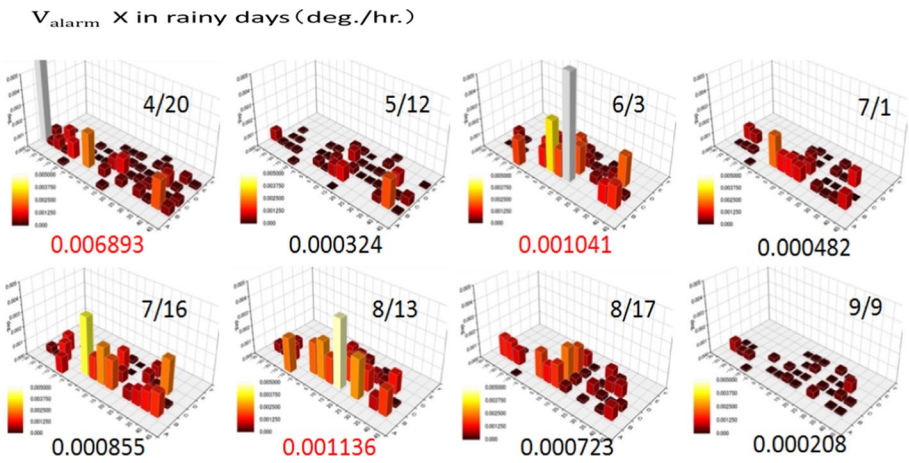

Fig. 33 Distribution of tilting rates during each rainfall day at the Manzawa site

The real-time risk evaluation for an unstable slope during rainfall based on principal component analysis becomes very important, it is the reason that our EWS is paying more attention to unstable slope movement.

A field engineer receives the rainfall warning first (rainfall warning issue), and then manages the safety by monitoring the movement of unstable slope (unstable slope creep movement issue). The movement on unstable slopes is the most important basis for issuing warnings.

4.1 Forecast of remaining time until landslide and slope failure

Table 2 and Fig. 34 summarize the results of the authors' slope monitoring projects since 2004, which have considered landslides, slope failure, collapse, and field experiments (Uchimura et al. 2015). The authors define landslides as events that require months or years until failure, slope failures as events that require days or weeks until failure, and collapses as events that only require hours until failure. Thus, the case of rainfall-induced slope failure is classified as a collapse. As previously mentioned, the brief amount of time until failure makes it difficult to select a relevant monitoring method. While the overall trend of the obtained data in Fig. 34 is similar to the Monkman–Grant model (Fig. 3) and the authors' previous empirical diagram (Fig. 9), it is further proposed that three different failure times may affect the plotted relationship.

In line with Eq. 1, the authors approximate the data in Fig. 34 using Eq. 3:

$$\log_{10} t_r = 0.306 - 0.597 \log_{10} \frac{d\alpha}{dt} \pm 0.6 \tag{3}$$

where tr denotes the time remaining until failure (hours) and $d\alpha/dt$ denotes the rate of the tilting angle (degree/hour). The prediction using Eq. 3 is indicated by the solid black line in Fig. 34. To further improve the time prediction, the following measures are considered:

Table 2 Summary of collapse case patterns

Site	Failure pattern	Slope geomorphology slope angle (degree)	Failure condition	Ground material
Dujiangyan, China	Field rainfall test	10–20	Artificial rainfall	Crushed stones with soil
SaiWanBa, China	Landslide	8–20	Rainfall	Clay and crushed stones
Hiyamizu, China	Slope failure	30	Rainfall	Strongly weathered granite
Sakada, Japan	Landslide	25	Erosion collapse	Sandstone mudstone mutual
Tagawa, Japan	Slope failure	25	Erosion collapse	Strongly weathered granite
Yofudo dam, Japan	Slope failure	30	Rainfall	Strongly weathered phyllite
Maleny, Australia	Landslide	8–12	Rainfall	Clay on sedimentary rock
Zhongpu, Taiwan	Large-scale collapse	10–25	Rainfall	Soil and conglomerate
Niimi, Japan	Slope failure	15–25	Rainfall	Pebble soil mixed with clay
Hachioji, Japan	Slope failure	15–25	Rainfall	Embankment soil
Shibata, Japan	Slope failure	25–35	Rainfall	Embankment soil on sedimentary rock
Soeda, Japan	Slope failure	15–25	Rainfall	Weathered tuff breccia
Miyagi, Japan	Slope failure	15–25	Earthquake, rainfall	Weathered tuff breccia
Aso, Japan	Landslip	30–35	Earthquake, rainfall	Volcanic pyroclastic flow deposits
Kochi, Japan	Erosion collapse	20–30	Rainfall	Rock mass slope
Bhutan	Slope collapse	25–35	Rainfall	Muddy schist

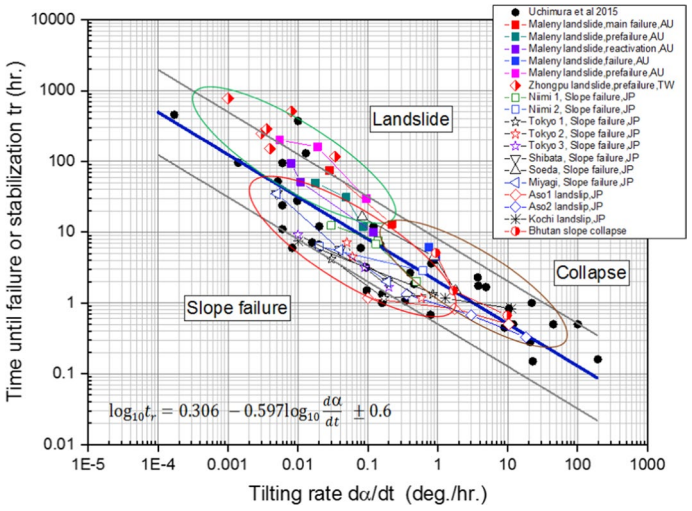

Fig. 34 Relationship between time remaining until failure and tilting rate based on field monitoring

i) Classification of events according to their type, such as landslide, slope failure, collapse, and so on.
ii) Classification according to slope materials, such as weathered granite, sedimentary rocks, soil in natural slopes, and so on.
iii) Classification according to geology, geography, and geomorphology, such as steep slope, smooth terrain, and so on.
iv) Classification according to the type of rainfall time history.

To implement these measures, a more extensive case history is required. At this moment, the different slope displacement rates in Fig. 34 suggest the following:

i) Landslides have sufficient time until failure, and emergency caution and warning alerts are appropriate measures.
ii) The failure of surface sediments (slope failure in Fig. 34) has several hours until failure if a warning is issued when the rate is 0.1°/hour.
iii) Collapse occurs suddenly and practical experience suggests that failure occurs within one hour or less. Hence, evacuation is not feasible and the reinforcement of the slope in advance using rock bolts, and so on, is advisable.

4.2 Early warning by using multi-point monitoring

Wang et al. (2017) proposed an early warning method based on single-sensor monitoring. Recently, the authors have extended the scope of slope monitoring to multi-point monitoring, which can capture both the spatial and temporal behavior of the entire slope. Additionally, multi-point monitoring can avoid erroneous warnings caused by very local slope movement and animal contact, among other causes of error. Thus, the reliability of early warning is improved.

The spacing between multiple sensors must be kept within a reasonable limit (a few meters to a few tens of meters, as in the practical cases discussed in this paper), and a new index of slope movement has to be proposed in the place of a single sensor's tilting rate, as in past practical cases. Certainly, the new index has to handle data at all monitoring points. Presently, the new index is assumed to be expressed as follows:

$$V_{\text{alarm}} = \sum_{i=1}^{n} \left(|V_i| \times \frac{A_i}{A} \times \partial_i \right) \tag{4}$$

where n is the total number of tilt sensors; V_{i} is the tilting rate (otherwise denoted as $\mathrm{d}\alpha/\mathrm{dt}$) in the slope direction of the ith sensor (°/hour); $\mathrm{A_i}$ is the area covered by the ith sensor; A is the area covered by the entire sensor array; ∂_{i} is the coefficient determined by the geology, geography, soil type, and vegetation conditions at the installation points. Moreover, the ∂_{i} coefficients regard the field conditions and their values are determined based on the results of geomaterial experiments and the assessment of geologists. Although this issue requires further investigation, $\partial_{\text{i}} = 1$ is currently used in practical situations.

5 Conclusions

The authors have been developing slope failure monitoring and early warning technology. This technology is characterized by the use of MEMS tilt sensors. In earlier versions, monitoring was conducted using a single sensor. However, a multi-sensor approach was implemented in a recent development. This paper introduces the most recent development of the authors' EWS based on data obtained from several sites and their interpretation. The following conclusions were drawn from this study:

(1) In the previous version of the technology, a caution alert was issued when the tilting rate exceeded 0.01°/hour, while a warning associated with an evacuation order was issued when the rate exceeded 0.1°/hour. These threshold values are based on practical experience, and have been validated by recently obtained monitoring results.
(2) In this paper, various monitoring cases are summarized. The linear relationship between the logarithm of the rate of the tilting angle of the sensors and the logarithm of the time remaining until slope failure was demonstrated. This relationship has an interesting similarity to the relationships suggested by the Monkman–Grant model and Saito's rheological interpretation of laboratory soil tests.
(3) The recent extension of monitoring to multi-point practice enables a more a detailed interpretation of slope behavior in the transient stage and up to the final failure.

Acknowledgements The authors gratefully acknowledge the support provided to this study by the Council for Science, Technology and Innovation, "Cross-ministerial Strategic Innovation Promotion Program (SIP), Infrastructure Maintenance, Renovation, and Management" (funding agency: NEDO), Sino-Japanese Intergovernmental International Cooperation in Science and Technology Innovation (Project Nos: 2021YFE0111900).

Funding The authors have not disclosed any funding.

Declarations

Conflict of interest Hereby, We "Lin Wang, Ichiro Seko, Makoto Fukuhara, Ikuo Towhata, Taro Uchimura, Shangning Tao" consciously assure that for the manuscript " Risk evaluation and warning threshold of unstable slope using tilting sensor array" the following is fulfilled:
(1) This material is the authors' own original work, which has not been previously published elsewhere. (2) The paper is not currently being considered for publication elsewhere. (3) The paper reflects the authors' own research and analysis in a truthful and complete manner. (4) The paper properly credits the meaningful contributions of co-authors and co-researchers. (5) The results are appropriately placed in the context of prior and existing research. (6) All sources used are properly disclosed (correct citation). Literally copying of text must be indicated as such by using quotation marks and giving proper reference. (7) All authors have been personally and actively involved in substantial work leading to the paper, and will take public responsibility for its content.
The violation of the Ethical Statement rules may result in severe consequences.
I agree with the above statements and declare that this submission follows the policies of Natural Hazards as outlined in the Guide for Authors and in the Ethical Statement.

References

Abeykoon T, Gallage C and Trofimovs J (2019) Optimisation of sensor locations for reliable and economical early warning of rainfall-induced landslides. In: 9th Int. Conf. on Geotechnique, Construction Materials and Environment, Tokyo, Japan. 20–22 November 2019, ISBN: 978–4–909106025 C3051. https://eprints.qut.edu.au/197046

Baum RL, Godt W (2010) Early warning of rainfall-induced shallow landslides and debris flows in the USA. Landslides 7(3):259–272. https://doi.org/10.1007/s10346-009-0177-0

Brunetti MT, Peruccacci S, Rossi M, Luciani S, Valigi D, Guzzetti F (2010) Rainfall thresholds for the possible occurrence of landslides in Italy. Nat Hazard 10(3):447–458. https://doi.org/10.1016/j.geomorph.2017.03.031

Caine Nel (1980) The rainfall intensity: duration control of shallow landslides and debris flows. Geogr Ann. Ser A, Phys Geograp 62(1/2):23. https://doi.org/10.2307/520449

Campbell RH (1975) Soil slips, debris flows, and rainstorms in the Santa Monica Mountains and vicinity, Southern California. US Geol Surv Prof Pap. https://doi.org/10.3133/pp851

Carlà T, Intrieri E, Di Traglia F, Nolesini T, Gigli G, Casagli N (2017) Guidelines on the use of inverse velocity method as a tool for setting alarm thresholds and forecasting landslides and structure collapses. Landslides 14:517–534. https://doi.org/10.1007/s10346-016-0731-5

Casagli N, Catani F, Ventisette C, Luzi G (2010) Monitoring, prediction and early warning using ground-based radar interferometry. Landslides 7(3):291–302. https://doi.org/10.1007/s10346-010-0215-y

UN-ISDR Developing early warning systems, a checklist: Third international conference on early warning (EWC III), 27–29 March 2006, Bonn, Germany-UNISDR. https://www.unisdr.org/2006/ppew/info-resources/ewc3/checklist/English.pdf

Endo T (1969) Probable distribution of the amount of rainfall causing landslides, Annual Report 1968, Hokkaido Branch, Government Forest Experiment Station, 122–136 (in Japanese)

Fukuzono T (1985) A new method for predicting the failure time of a slope. In: Proceedings of the 4th International Conference and Field Workshop on Landslides, Tokyo, Japan, 23–31 August 1985; Japan Landslide Society: Tokyo, Japan, 1985; pp 145–150

Kayen R, Pack RT, Bay J, Sugimoto S, Tanaka H (2006) Terrestrial-LIDAR visualization of surface and structural deformations of the 2004 Niigata Ken Chuetsu Japan. Earthq Spectra 22(S1):S147–S162

Lee W F, Liao HJ, Wang CH (2013) Failure analysis of a highway dip slope slide. 4th Int. Seminar on Forensic Geotechnical Engineering. Bangalore, 325–338

Medina-Cetina Z, Nadim F (2008) Stochastic design of an early warning system. Georisk Assess. Manage Risk Eng Syst Geohazards 2:223–236. https://doi.org/10.1080/17499510802086777

Monkman FC, Grant NJ (1956) An empirical relationship between rupture life and minimum creep rate in creep rupture tests. Procee, Am Soc Testing Mater 56(1956):593–620

Nakai S, Kaibori M, Sasaki Y, Moriwaki T (2007) Applicability of a new rainfall index R' for recent cases and proposal of the method for warning against sediment-related disaster. J Jpn Soc Eros Control Eng 60(1):37–42

Nolasco-Javier D, Kumar L, Tengonciang AMP (2015) Rapid appraisal of rainfall threshold and selected landslides in Baguio. Philipp Nat Hazards 78(3):1587–1607. https://doi.org/10.1007/s11069-015-1790-y

Onodera T, Yoshinaka R, Kazama H (1974) Slope failures caused by heavy rainfall in Japan. J Jpn Soc Eng Geol 15(4):191–200

Osanai N, Shimizu T, Kuramoto K, Kojima S, Noro T (2010) Japanese early-warning for debris flows and slope failure using rainfall indices with radial basis function network. Landslides 7(3):325–338. https://doi.org/10.1007/s10346-010-0229-5

Piciullo L, Gariano SL, Melillo M, Brunetti MT, Peruccacci S, Guzzetti F, Calvello M (2017) Definition and performance of a threshold-based regional early warning model for rainfall-induced landslides. Landslides 14(3):995–1008. https://doi.org/10.1007/s10346-016-0750-2

Saito M and Uezawa H (1961) Failure of soil due to creep. In: Proceedings of the 5th international conference on soil mechanics and foundation engineering. Vol.1, pp 315–318 (Paris), https://www.issmge.org/uploads/publications/1/40/1961_01_0054.pdf

Saito M (1965) Forecasting the time of occurrence of a slope failure. In: Proceedings of the 6th international conference on soil mechanics and foundation engineering. Vol. 2, pp 537–541 (Montréal), https://www.issmge.org/uploads/publications/1/39/1965_02_0116.pdf

Sartori M, Baillifard F, Jaboyedoff M, Rouiller JD (2003) Kinematics of the 1991 Randa rockslides (Valais, Switzerland). Nat Hazards Earth Syst Sci, Copernic Publ Behalf Eur Geosci Union 3(5):423–433. https://doi.org/10.5194/nhess-3-423-2003

Segalini A, Valletta A, Carri A (2018) Landslide time-of-failure forecast and alert threshold assessment: a generalized criterion. Eng Geol 245:72–80. https://doi.org/10.1016/j.enggeo.2018.08.003

Segoni S, Piciullo L, Gariano SL (2018) A review of the recent literature on rainfall thresholds for landslide occurrence. Landslides 15:1483–1501. https://doi.org/10.1007/s10346-018-0966-4

Terlien MTJ (1998) The determination of statistical and deterministic hydrological landslide-triggering thresholds. Environ Geol 35(2–3):124–130. https://doi.org/10.1007/s002540050299

Tharindu A, Chaminda G, Dareeju (2018) Real-time monitoring and wireless data transmission to predict rain induced landslides in critical slopes. Aust Geomech J 53(3):61–76

Uchimura T, Towhata I, Wang L, Nishie S, Yamaguchi H, Seko I, Qiao JP (2015) Precaution and early warning of surface failure of slopes by using tilt sensors. Soils Found 55(5):1086–1099. https://doi.org/10.1016/j.sandf.2015.09.010

Wang L, Nishie S, Su L, Uchimura T, Tao S, and Towhata I (2017) Proposed early warning system of slope failure by monitoring inclination changes in multipoint tilt sensors. In: 19th international conference on soil mechanics and geotechnical engineering, Seoul, South Korea, 2215–2218

Yin YP (2010) Integration of GPS with InSAR to monitoring of the Jiaju landslide in Sichuan. China Landslides 7(3):359–365. https://doi.org/10.1007/s10346-010-0225-9

Authors and Affiliations

Lin Wang[1] · Ichiro Seko[1] · Makoto Fukuhara[1] · Ikuo Towhata[2] · Taro Uchimura[3] · Shangning Tao[1]

Ichiro Seko
seko@ckcnet.co.jp

Makoto Fukuhara
fukuhara@ckcnet.co.jp

Ikuo Towhata
towhata.ikuo.ikuo@gmail.com

Taro Uchimura
uchimurataro@mail.saitama-u.ac.jp

Shangning Tao
tao.s@ckcnet.co.jp

[1] Chuo Kaihatsu Corporation, Address: 3-13-5 Nishi-Waseda, Shinjuku-Ku, Tokyo 169-8612, Japan

[2] University of Tokyo, Tokyo, Japan

[3] Saitama University, Saitama City, Japan